

## THE CELSIUS/WASA $4\pi$ DETECTOR FACILITY\*

C. BARGHOLTZ<sup>o</sup>, R. BILGER<sup>c</sup>, M. BLOM<sup>a</sup>, D. BOGOSLAWSKY<sup>d</sup>  
 A. BONDAR<sup>f</sup>, W. BRODOWSKI<sup>c</sup>, H. CALEN<sup>b</sup>, H. CLEMENT<sup>c</sup>  
 L. DEMIRÖRS<sup>m</sup>, V. DUNIN<sup>d</sup>, C. EKSTRÖM<sup>b</sup>, K. FRANSSON<sup>a</sup>  
 C-J. FRIDEN<sup>b</sup>, J. GREIFF<sup>a</sup>, L. GUSTAFSSON<sup>a</sup>, B. HÖISTAD<sup>a</sup>  
 M. JACEWICZ<sup>a</sup>, J. JOHANSON<sup>a</sup>, A. JOHANSSON<sup>a</sup>, T. JOHANSSON<sup>a</sup>  
 A. KHOUKAZ<sup>n</sup>, K. KILIAN<sup>g</sup>, N. KIMURA<sup>k</sup>, I. KOCH<sup>a</sup>, G. KOLACHEV<sup>f</sup>  
 M. KOMOGOROV<sup>d</sup>, S. KULLANDER<sup>a</sup>, A. KUPŚC<sup>b</sup>, L. KURDADZE<sup>f</sup>  
 A. KUZMIN<sup>f</sup>, A. KUZNETSOV<sup>d</sup>, B. LUNDSTRÖM<sup>b</sup>, P. MARCINIEWSKI<sup>a</sup>  
 B. MARTEMYANOV<sup>j</sup>, B. MOROSOV<sup>d</sup>, A. NAWROT<sup>e</sup>, B.M.K. NEFKENS<sup>l</sup>  
 G. NORMAN<sup>b</sup>, W. OELERT<sup>g</sup>, S. ORESHKIN<sup>f</sup>, Y. PETUKHOV<sup>d</sup>, S. POMP<sup>b</sup>  
 A. POVTOREJKO<sup>d</sup>, K. PRZESTRZELSKA<sup>a</sup>, J. PÄTZOLD<sup>c</sup>, D. REISTAD<sup>b</sup>  
 R.J.M.Y. RUBER<sup>b</sup>, V. SANDUKOVSKY<sup>d</sup>, W. SCOBEL<sup>m</sup>, T. SEFZICK<sup>g</sup>  
 S. SEWERIN<sup>b</sup>, V. SIDOROV<sup>f</sup>, B. SHWARTZ<sup>f</sup>, V. SOPOV<sup>j</sup>, J. STEPANIAK<sup>e</sup>  
 A. SUKHANOV<sup>f</sup>, P. SUNDBERG<sup>a</sup>, V. TCHERNYCHEV<sup>j</sup>, P-E. TEGNER<sup>o</sup>  
 P. THÖRNGREN ENGBLOM<sup>a</sup>, V. TIKHOMIROV<sup>d</sup>, A. TUROWIECKI<sup>i</sup>  
 G. WAGNER<sup>c</sup>, U. WIEDNER<sup>a</sup>, Z. WILHELMI<sup>i</sup>, A. YAMAMOTO<sup>k</sup>  
 H. YAMAOKA<sup>k</sup>, J. ZABIEROWSKI<sup>h</sup>, A. ZERNOV<sup>d</sup>, J. ZLOMAŃCZUK<sup>a</sup>

<sup>a</sup>ISV, Uppsala, Sweden; <sup>b</sup>TSL, Uppsala, Sweden; <sup>c</sup>Tübingen University, Germany;  
<sup>d</sup>JINR, Dubna, Russia; <sup>e</sup>INS, Warsaw, Poland; <sup>f</sup>BINP, Novosibirsk, Russia; <sup>g</sup>IKP,  
 KFA, Jülich, Germany; <sup>h</sup>INS, Łódź, Poland; <sup>i</sup>Inst. of Exp. Phys., Warsaw Univ.,  
 Poland; <sup>j</sup>ITEP, Moscow, Russia; <sup>k</sup>KEK, Tsukuba, Japan; <sup>l</sup>UCLA, Los Angeles,  
 USA; <sup>m</sup>Hamburg University, Germany; <sup>n</sup>University of Münster, Germany;  
<sup>o</sup>Stockholm University, Sweden

*(Received July 13, 2000)*

A new experimental setup for light-ion physics located at the CELSIUS storage ring of The Svedberg Laboratory in Uppsala is now in the commissioning phase. It consists of an internal pellet target station and the WASA detector covering a solid angle close to  $4\pi$  steradians. Its central part is optimized to measure energies of electrons and photons for energies up to 600 MeV. The setup and the initial physics programme is presented as well as the status of the commissioning.

PACS numbers: 13.60.Le, 13.20.Jf

---

\* Presented by A. Kupśc at the Meson 2000, Sixth International Workshop on Production, Properties and Interaction of Mesons, Cracow, Poland, May 19–23, 2000.

## 1. Introduction

The CELSIUS/WASA, a facility for medium energy light-ion physics at The Svedberg Laboratory in Uppsala, is now in the commissioning phase. The experiment is designed to study some rare decays of eta such as  $\eta \rightarrow e^+e^-$  and  $\eta \rightarrow \pi^0 e^+e^-$  with anticipated branching ratios  $\approx 10^{-9}$ . In addition a wide range of meson production reactions are accessible and can be studied with high accuracy. The necessary high luminosity of around  $10^{32} \text{ cm}^{-2}\text{s}^{-1}$  is achieved by using a newly developed target system that provides small frozen hydrogen spheres (pellets) as internal targets in the CELSIUS accelerator. At present the maximum energy for protons is 1360 MeV and after a planned upgrade the maximum energy will be increased to 1900 MeV. The main parameters of the CELSIUS proton beams are listed in Table I.

TABLE I

Some parameters of the CELSIUS storage ring.

Proton beam parameters:	uncooled	cooled
Maximum kinetic energy	1360 MeV	550 MeV
Beam diameter	10 mm	1 mm
Relative momentum spread	$2 \times 10^{-3}$	$2 \times 10^{-4}$
Number of stored protons	$5 \times 10^{10}$	$1 \times 10^{10}$
Beam current	27 mA	4.5 mA

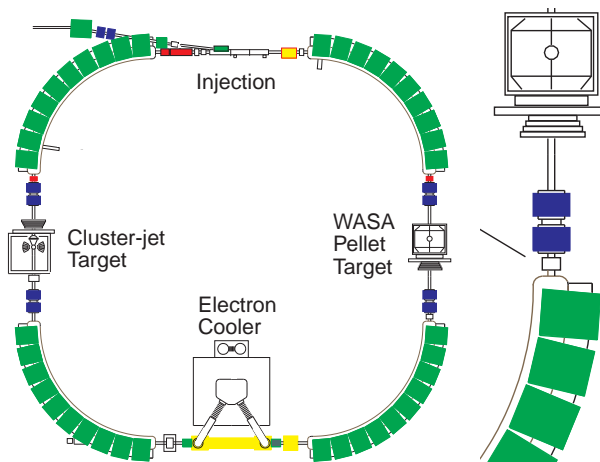


Fig. 1. CELSIUS storage ring and the CELSIUS/WASA facility.

## 2. Pellet target system

The pellet target system is presented schematically on the left side of figure 2. A jet of liquid hydrogen is broken up into droplets by a vibrating

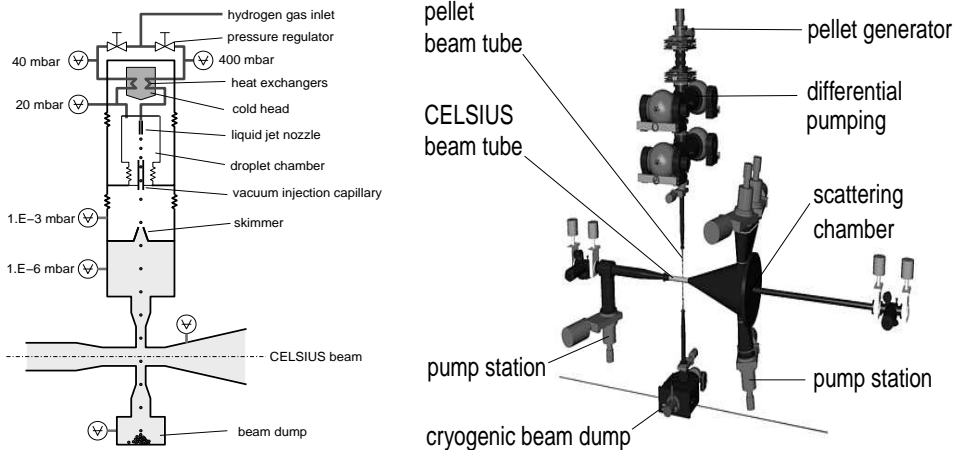


Fig. 2. Schematic view of the pellet target system.

of an injection nozzle. The droplets freeze by evaporation in the droplet chamber and form pellets that are injected into vacuum. After collimation, the pellets are directed through a thin long tube into the scattering chamber. This arrangement provides the necessary space to put a  $4\pi$  detection system around the interaction region. The pellet target thickness of up to  $5 \times 10^{15}$  atoms/cm<sup>2</sup> gives acceptable half-lives of the circulating ion beam as well as acceptable vacuum conditions. Some parameters of the pellet target are listed in Table II. The small size of the pellets ensures that the probability of secondary interactions inside of the target is low. The pellet system was developed in Uppsala [1] and has been successfully tested at CELSIUS with hydrogen and deuterium pellets [2].

TABLE II

Some parameters of the pellet target system.

Parameters of the pellet target:	
Pellet diameter	35 $\mu\text{m}$
Max pellet frequency	70 kHz
Pellet stream divergence	0.04 $^\circ$
Effective target thickness	$10^{15} - 10^{16}$ atoms/cm <sup>2</sup>
Beam diameter	2–4 mm

### 3. Overview of the WASA $4\pi$ detector

The detector consists of three main parts: a central detector, a forward detector and a zero-degree spectrometer. A cross section of the central and the forward part is presented in figure 3.

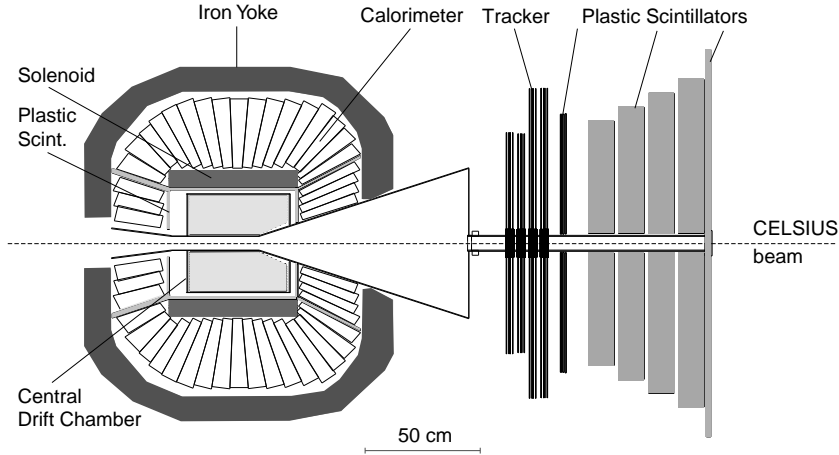


Fig. 3. Cross section in the plane of the CELSIUS beam of the WASA  $4\pi$  detector.

The forward detector covers scattering angles from  $3^\circ$  to  $18^\circ$ . Its purpose is the measurement of charged target recoil particles and scattered projectiles. The central part of the detector is optimized for meson decay products like electrons, photons and charged pions. It consists of a cylindrical drift chamber, placed inside of a superconducting solenoid, and of an electromagnetic calorimeter of CsI crystals. Fast signals for trigger purposes are provided by a plastic scintillator barrel enclosing the drift chamber. The zero-degree spectrometer is positioned in the accelerator quadrant downstream of the pellet target and used for measurement of deuterons,  $^3\text{He}$  and  $^4\text{He}$  particles scattered at angles below  $1^\circ$  (Table III).

TABLE III

Parameters of the Zero-degree spectrometer.

Sensitive Material	CsI and high purity germanium
Range of scattering angle	$0^\circ$ - $0.85^\circ$
Rigidity range ( $Zp/p_{\text{beam}}$ )	0.3-0.95
Energy resolution for helium (CsI variant)	$12\% / \sqrt{E[\text{MeV}]}$ (FWHM)

The forward detector, described in detail in [3], consists of several planes of plastic scintillators. Four layers, 11cm thick each, are used to measure the energy of charged particles. The other plastic detectors are used for trigger and for particle identification. Charged particles tracking is provided by several layers of thin walled straw tubes. The main parameters are listed in Table IV.

TABLE IV  
Parameters and typical performance of the forward detector.

Scattering angle resolution	< 0.2° (FWHM)
Energy resolution $\Delta E/E$	3 % (FWHM)
Thickness	$1X_0 \sim 50 \text{ g/cm}^2$
Maximum kinetic energy for stopping	
charged pions	170 MeV
protons	300 MeV
deuterons	400 MeV
alpha particles	900 MeV

In the central detector, charged particles tracks are measured by the 17 layers of individual thin drift tubes (1738 in total). The central drift chamber covers scattering angles between  $24^\circ$  to  $159^\circ$ . The momentum resolution with magnetic field of 1 Tesla for different particles is given in Table 5. The superconducting solenoid has to have walls as thin as possible in order to minimize disturbance on the particle energy determination in the electromagnetic calorimeter. The wall thickness corresponds to 0.18 radiation lengths only, a record for this kind of magnets. The plastic scintillator barrel provides  $\Delta E$  information for charged particle identification.

TABLE V  
Parameters and typical performance of the central detector.

Maximum kinetic energy for stopping:	
charged pion	190 MeV
proton	400 MeV
deuteron	450 MeV
Energy resolution for:	
100 MeV photon	10 % (FWHM)
stopped charged particles	3 % (FWHM)
Momentum resolution for:	
electrons (20 – 600 MeV/c)	1 % (FWHM)
$\pi^\pm$ and $\mu$ (100 – 600 MeV/c)	4 % (FWHM)
protons (200 – 800 MeV/c)	5 % (FWHM)

The electromagnetic calorimeter covers scattering angles from  $20^\circ$  to  $169^\circ$  (96% of  $4\pi$  steradians). Its primary purpose is to detect and measure photons, electrons and positrons with energies up to 600 MeV. The calorimeter consists of 1012 sodium-doped CsI scintillating crystals. The crystals are shaped as truncated pyramids and supported on the back end only. They are placed in 24 layers along the beam. A layer in the central part consists of 48 identical crystals. The length of the crystals vary from 30 cm ( $16.2 X_0$ ) in the central part to 25 cm in the forward and 20 cm in the backward part. Each crystal is optically coupled by light guides to the photomultiplier placed outside of the iron yoke and supplied with an optical fiber providing light pulser signals for monitoring and calibration purposes. The use of photomultipliers provides a clear advantage in terms of energy resolution and timing.

#### 4. Physics programme

The forward detector and 112 crystals of the calorimeter were previously used for six years in experiments at the cluster-jet target. Studies of near threshold  $\pi^0$  and  $\eta$  meson production in nucleon–nucleon collisions as well as  $\pi^+\pi^-$  pair production were made. Some of the reaction channels were measured for the first time [4–9]. Other items of interest were bremsstrahlung, deuteron break-up mechanism, and searches for dibaryon states.

The studies of light mesons production from  $pp$  and  $pd$  interactions will be continued with high acceptance conditions what will allow for efficient identification of mesons production events over a large kinematical range. The possibility to identify some heavier mesons using different decay modes will help to control systematic errors. For example the  $\eta$  meson could be identified by its decay into two photons as well as by its decay into three neutral pions.

Figure 4 shows some mesonic final states that could be studied at CELSIUS in  $pp$ ,  $pd$  and  $dd$  interactions. The solid horizontal line represent the present momentum limit of CELSIUS and the dashed line the limit after the planned upgrade. The upgrade will open new physics possibilities, like  $\eta'$  and  $\phi$  meson production studies.

The collaboration has an extended programme of studies of rare decays of the  $\eta$  meson. This will allow to search for violations of fundamental symmetries and to provide crucial tests of Chiral Perturbation Theory. The most important production reactions of the eta meson for the decay programme are summarized in Table VI. Eta mesons for the precise measurements of the not so rare  $\eta \rightarrow 3\pi$  or  $\eta \rightarrow \pi^0\gamma\gamma$  decays can be produced in  $pd \rightarrow {}^3\text{He}\eta$  reaction close to the threshold where  ${}^3\text{He}$  is measured in the zero-degree spectrometer. For the very rare decays with branching ratios of  $10^{-8}$  the reaction  $pp \rightarrow pp\eta$  at 1360 MeV must be used.

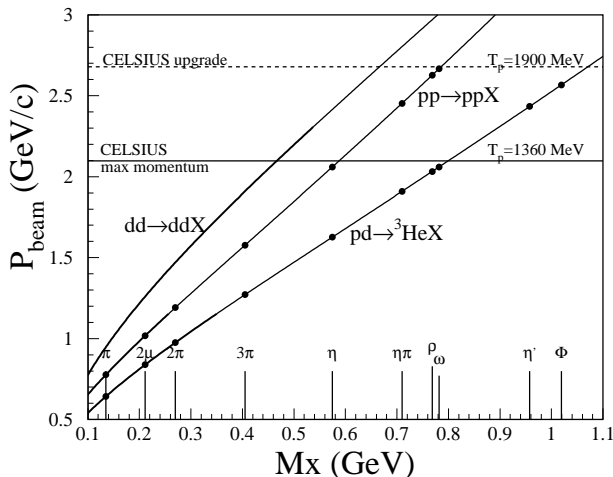


Fig. 4. Particles that can be studied at CELSIUS/WASA.

TABLE VI

Production reactions for the  $\eta$  decay programme. Rates are estimated for a luminosity of  $10^{32} \text{ cm}^{-2}\text{s}^{-1}$ .

Reaction	$pp \rightarrow pp\eta$	$pd \rightarrow {}^3\text{He}\eta$	
$T_p$ [MeV]	1360	1500	895
Cross section	$5 \mu\text{b}$	$25 \mu\text{b}$	$0.5 \mu\text{b}$
Useful rate ( $\eta\text{s/day}$ )	$2 \times 10^7$	$1 \times 10^8$	$2 \times 10^6$
Tagging resolution (FWHM)	5 MeV	10 MeV	<1 MeV

## 5. Status of the commissioning

The main parts of the detector have been installed at CELSIUS. The pellet system is being tuned for proper performance with the CELSIUS beam. Tests of the individual detector elements were done during the installation phase. Now readout electronics is being installed and the different detector systems are tuned in regular runs. In 1999, runs were carried through with most of the plastic scintillators and an increasing number of CsI crystals connected (now all crystals are connected). The forward detector with its drift chambers were verified to work properly. The basic performance of the central drift chambers were studied and a few layers were tested. The data acquisition system and digitizing electronics for the large amount of channels and the anticipated high luminosity runs are being developed. The goal is to be able to start regular meson production runs in the fall using most of the detector.

## REFERENCES

- [1] B. Trostell, *Nucl. Instrum. Methods* **A362**, 41 (1995).
- [2] C. Ekström *et al.*, *Nucl. Instrum. Methods* **A371**, 572 (1996).
- [3] H. Calén *et al.*, *Nucl. Instrum. Methods* **A379**, 57 (1996).
- [4] A. Bondar *et al.*, *Phys. Lett.* **B356**, 8 (1995).
- [5] H. Calén *et al.*, *Phys. Lett.* **B366**, 39 (1996).
- [6] H. Calén *et al.*, *Phys. Rev. Lett.* **79**, 2642 (1997).
- [7] H. Calén *et al.*, *Phys. Rev.* **C80**, 2667 (1998).
- [8] H. Calén *et al.*, *Phys. Lett.* **B458**, 190 (1999).
- [9] J. Złomańczuk *et al.*, *Phys. Lett.* **B436**, 251 (1998).